Nanomechanical Energy Transfer and Resonance Effects in Single-Walled Carbon Nanotubes

P. Alex Greaney and Jeffrey C. Grossman*

Center of Integrated Nanomechanical Systems, University of California at Berkeley, Berkeley, California 94720, USA

(Received 15 June 2006; published 22 March 2007)

Molecular dynamics simulations are employed to elucidate the important factors in mechanical energy transfer between carbon nanotubes. Our calculations show that sharp resonance effects allow for near complete and highly efficient energy transfer. In addition, the weak coupling between two nanotubes sets the time scale for the energy transfer. The simulations provide the mechanistic basis for a theoretical description of lattice vibration mediated heat flow in nanoscale materials.

DOI: 10.1103/PhysRevLett.98.125503 PACS numbers: 63.22.+m, 61.46.Fg, 81.07.De

Understanding thermal transport in nanoscale materials is of profound importance for the thermal management of the next generation of microelectronic, photovoltaic, and thermoelectric devices. Carbon nanotubes (CNTs) are endowed with a variety of unusual vibrational properties that show potential for thermal management applications [1–3]. Thermal transport in single-walled carbon nanotubes (SWNTs) has been predicted to be ballistic in tubes of moderate length [4] and at low temperatures the thermal conductance is quantized [5]. Although most experimental work has focused on understanding heat transfer *along* the axis of a nanotube, recent experiments [6,7] indicate that thermal conductance in ropes and mats of SWNTs is limited by the transfer of energy *between* tubes.

In this Letter, molecular dynamics (MD) simulations are employed to elucidate the mechanisms of vibrational energy transfer between nanoscale objects. Our calculations show that energy is exchanged between two nanotubes efficiently with modes in resonance, and that a strong relationship exists between the rate of kinetic energy transfer from one tube to another and the strength of the intertube van der Waals (vdW) interaction. This dependence establishes two distinct time scales that play a fundamental role in nanomechanical energy transfer. Our simulations illustrate a third critical time scale set by a nonlinear mechanism of internal scattering. We combine these factors to form the basis of a model of heat transfer between nanoscale objects.

Classical MD simulations were performed using the reactive empirical bond order potential [8] for nearest-neighbor bonds, and a Lennard-Jones potential for longer range vdW bonding. As a prototypical system to study heat transfer at the nanoscale, two single-walled CNTs were arranged parallel to each other with periodic conditions imposed along the tube axes. In contrast to previous MD studies of heat transfer [2,9,10] we focus on the transfer of energy between stationary vibrational modes rather than transport over distance by traveling wave packets [11]. The general procedure for a typical simulation was as follows: first the coordinates of the tubes (and the width of the computational cell) were optimized to better than 10^{-5} eV/Å. Second, specific phonon modes in one of the tubes (referred to as tube A) were displaced, while the other tube (B) was held fixed. In all cases simulations were performed of (10, 0) tubes each containing 400 atoms in the unit cell (10 turns of the tube [14]). The selected modes were excited with an energy equivalent to 18 K. Simulations were conducted in the microcanonical ensemble, and the system was evolved with a predictor-corrector integration scheme using a time step of 0.2 fs.

If the breathing mode of tube A is initially excited, the transfer of energy between tubes can be seen directly from the oscillation of the tube radii, shown in Fig. 1. Immediately after it is released the radius of tube A oscillates with frequency 8.6 THz (in good agreement with *ab initio* calculations [15], indicating that the tube is in the harmonic regime). Over a longer time scale, the amplitude of the breathing oscillation in tube A decays while the breathing mode in tube B becomes active until around 8.7 ps (or 75 breathing oscillations), at which point tube A has transferred almost all of its kinetic energy into the breathing mode of tube B. One might expect this pattern of resonant energy transfer between the breathing modes to continue with the energy transferring back to tube A; however, after 9 ps a more complicated behavior occurs in which other vibrational modes become excited.

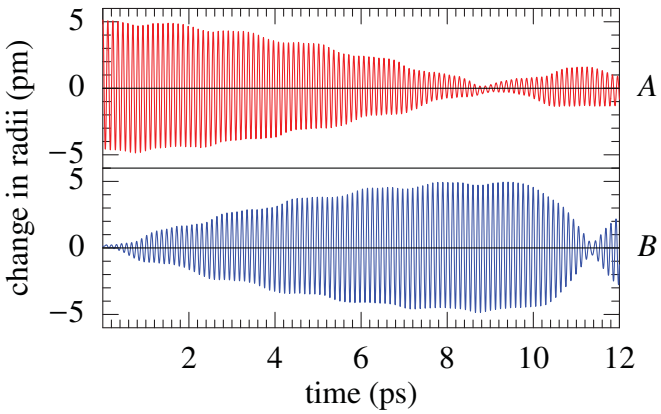

FIG. 1 (color). Change in the radius of tubes A (red) and B (blue) as a function of time.

In order to understand the mechanism for energy exchange as well as the energy scattering at 9 ps, we have computed the specific energy distribution *dynamically* among the phonon modes in each tube, shown in Fig. 2. The energy, $E_i(t)$, in the ith mode at time t is given by the projection of the atomic displacements and velocities onto the ith eigenmode of a CNT at equilibrium,

$$E_i(t) = \frac{\kappa_i}{2}[\boldsymbol{u}(t) \cdot \boldsymbol{\eta}_i]^2 + \frac{m}{2}[\boldsymbol{v}(t) \cdot \boldsymbol{\eta}_i]^2. \quad (1)$$

The two terms are the potential and kinetic energy of the mode where m is mass, and $\boldsymbol{v}(t)$ and $\boldsymbol{u}(t)$ are the (phase space) velocity of the tube and its displacement from equilibrium, respectively. The set of unit eigenvectors, $\boldsymbol{\eta}_i$, and the stiffness of the tube, κ_i, along this direction in phase space were determined *a priori* using the frozen phonon method.

While the energy transfer between breathing modes is clearly evident in Fig. 2, it can be seen that other phonon modes are excited throughout the simulation. In particular, modes at 1.2, 3.5, and 11.7 THz are excited intermittently from the start, and later modes at 4.3 THz become active. Additionally, the tube-tube interaction permits an intertube oscillation with a period of 1.6 ps (which is 1.9 times slower than the softest intratube mode). The activity of this coupling is indicated in Fig. 2 by the separation of the tubes' centers of mass, plotted along the time axis. The intertube oscillation is highly nonlinear with motion similar to a bouncing rubber ball: as the tubes come together the hard repulsive part of the vdW interaction causes the tubes to flatten elastically. The elastic energy associated with this deformation shows up in Fig. 2 as the periodic lumps in step with the tube oscillation at frequencies 1.2, 3.5, and 11.7 THz which correspond to the twofold and threefold symmetric radial modes and a mirror-symmetric cyclops mode [16].

As a rudimentary model of the energy exchange between tubes we consider the interaction between pairs of modes in each tube independently as two weakly coupled harmonic oscillators with equations of motion,

$$m_i\ddot{u}_i(t) = -\kappa_i u_i(t) + \kappa_c[u_{3-i}(t) - u_i(t)]. \quad (2)$$

Here m_i, κ_i, and u_i are the mass, stiffness, and displacement of the ith oscillator (the identifier i can be 1 or 2), the over dots represent the time derivative, and κ_c is the stiffness of the coupling. The resonant exchange between the breathing modes can be represented by considering the case where the two oscillators are identical. This composite system has two eigenmodes: one in which both oscillators move in the same direction with angular frequency $\sqrt{\kappa_1/m_1}$, and the other in which the oscillators move in opposite directions with angular frequency $\sqrt{(\kappa_1 + 2\kappa_c)/m_1}$. As these two hybrid modes beat in and out of phase the oscillators are alternately stilled and excited, and in the case that the amplitudes of the eigenmodes are equal, all of the vibrational energy is shuttled from one oscillator to the other. Similarly, the (almost) complete reversible transfer of energy observed in our MD simulations occurs because the initial configuration of the tubes is equally composed of both hybridizations of the two breathing modes.

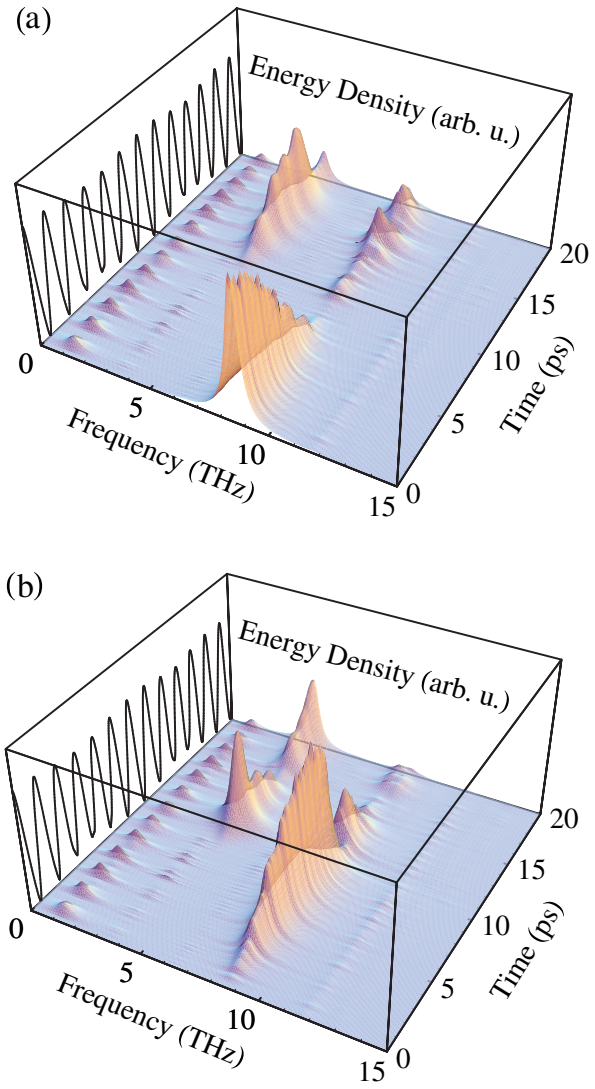

FIG. 2 (color). Temporal evolution of the distribution of energy [Eq. (1)] in vibrational modes of tubes A (top) and B (bottom). The tube-tube separation is plotted (in arbitrary units) along the time axis.

In this simple model the time taken for the energy to transfer from one oscillator to the other is one half of the beat period, ω_{beat}, of the two normal (hybrid) modes of the composite system. This gives the ratio of the energy transfer time relative to the oscillator period of $[2(\sqrt{1+2\gamma} - 1)]^{-1}$, where $\gamma = \frac{\kappa_c}{\kappa_1}$ is the dimensionless coupling strength. From this analysis we expect modes with lower frequencies to exchange energy more rapidly, a trend consistent with the transmission coefficient of phonons across an acoustic impedance mismatched boundary [17,18]. Intuitively, this makes sense as lower frequency modes experience larger deformations than higher frequency

modes with the same energy and so would interact more strongly; in turn, this implies that contacting bodies of different temperatures exchange energy fastest through the low frequency modes.

The results shown in Figs. 1 and 2 demonstrate a highly efficient energy transfer from the radial breathing mode of one tube into that of another identical tube (i.e., the modes are perfectly in resonance). By simulating the same CNT system but altering the mass of the atoms in tube B we explore the sharpness of this resonant behavior. Fig. 3(a) shows how the peak fraction of energy transferred into the breathing mode of tube B in the first 8.7 ps ($q_{\max}$) changes as its frequency is varied. The peak is narrow with a width at half maximum of around 2% (i.e., ~5 wave numbers), implying that for the breathing mode adjacent tubes will only interact resonantly if their radii differ by less than 2%. In the simple coupled oscillator model the transfer efficiency is obtained from the ratio of the maximum transferable energy to the total energy in the system. For small coupling γ this shows a peak width that goes as $\sim 2\gamma$. An excellent fit to the central peaks in Fig. 3 is found for $\gamma = 0.008$, in good agreement with the prediction from the energy transfer time.

The stiffness of the coupling between the ith and jth modes of the two tubes is the change in the force felt by the jth mode of one tube caused by the displacement of the ith mode in the other tube. The strength of the coupling depends on the projection of the intertube force onto the modes of the contacting bodies, and thus is sensitive to the geometry of the participating modes. While heat flow between contacting bulk solids must be channeled through surface-localized modes, all the modes of single-walled CNTs are by definition surface modes, and so in principal the total (vibrational) specific heat of the tube has a direct path for exchange between tubes. Coupling is stronger for modes with radial displacements than for modes with tangential or longitudinal displacements. Figure 3(b) demonstrates that as the mass of the atoms in tube B is changed to bring its fourfold radial mode into resonance with tube A's breathing mode, the coupling is sufficient to allow significant exchange of energy. The importance of radial

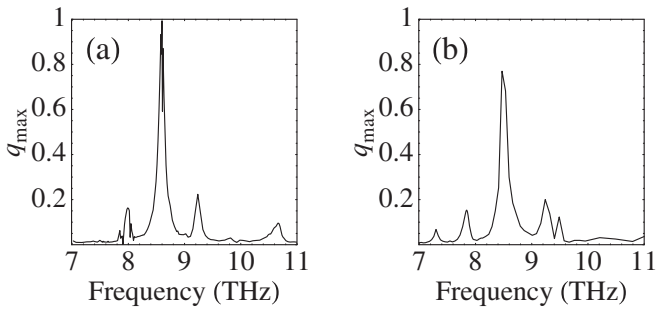

FIG. 3. Transfer efficiency ($q_{\max}$, see text) of the vibrational energy from the breathing mode of tube A into (a) the breathing mode and (b) the fourfold symmetric radial mode of tube B. The frequency of the modes in tube B are varied by altering the mass of its atoms.

modes, in conjunction with the sharp resonant frequency dependence, implies that in a composite nanomechanical system, the normal modes of the constitutive objects will only interact with the few modes in the adjoining objects that are close in frequency and share geometrical overlap. This justifies the assumption inherent in the simple oscillator model that coupling between pairs of modes may be considered individually.

Striking in Fig. 3 are the satellite peaks in $q_{\max}$ that bracket the resonant peaks. Here tube A's breathing mode excites modes with which it is not in resonance. The origin of this effect is the intertube bounce. In their equilibrium configuration the tubes are distorted by the vdW interaction. As the tube spacing vacillates, this distortion changes, modulating the coupling stiffness, κ_c, at the frequency of the tube-tube vibration, ω_{tt}. Evidence of this is seen in Fig. 2 where the resulting fluctuation in the energy transfer rate leaves ripples (in step with the intertube bounce) in the breathing component of the spectrum. Including the first Fourier component of the bounce in the coupling so that $\kappa_c = \langle \kappa_c \rangle + k_1 \cos(\omega_{\mathrm{tt}} t)$ in Eq. (2) gives terms with the form $k_1 \cos[(\omega_i \pm \omega_{\mathrm{tt}})t]$. As changing the mass of tube B also changes ω_{tt}, the satellite peaks are not symmetrically positioned. Accounting for this, the model predicts the first satellites to appear at frequencies of 8.0 and 9.3 THz for the breathing mode, and 7.9 and 9.4 THz for the fourfold mode, which are in good agreement with the MD results.

We now examine the origin of the sudden scattering of energy out of the breathing mode at roughly 9 ps, as shown in Figs. 1 and 2. Specifically, the breathing mode in tube B transfers its energy into the four degenerate modes with frequency closest to one half that of the breathing mode—which then transfers it back again. This exchange is a *resonant* anharmonic effect; the asymmetry of the breathing mode permits it and the half-frequency modes (which are symmetric) to "talk" to each other resonantly. This half-frequency exchange is observed for a single tube in isolation and the period of energy exchange decreases with increasing total energy in the mode pair. Resonant anharmonic exchange of energy can occur between any pair of modes whose frequencies differ by a factor of 2, provided the high frequency mode is asymmetric (breaks parity) and the low frequency mode is not. Hence, the breathing mode does not exchange energy with the double frequency modes for this system.

In Fig. 2 it can be seen that once the half-frequency modes are excited in tube B, they transfer their energy resonantly with the equivalent modes in tube A. This hints at the fundamental origin for the dissipation of vibrational energy in nanomechanical systems. Although the transfer mechanisms discussed in this work are reversible, energy is redistributed irreversibly by the continued branching of the energy pathway. We can combine the energy transfer mechanisms elucidated by the MD study into a picture of heat flow between two nanoscale objects with different thermal energies. In these small systems the macroscopic description of heat flux by a gas of traveling wave packets

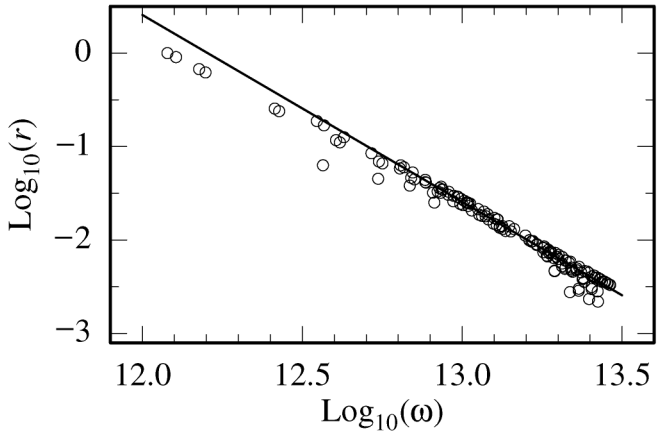

FIG. 4. Log-log plot of mode transmittance r of the radial modes as a function of mode frequency. The solid with slope of -2 is plotted for comparison.

is not appropriate. Instead, we assume pairs of resonant modes to exchange energy deterministically (according to the coupled oscillator model) over the time interval τ_s between internal scattering events that disturb these modes. Averaging over all trajectories of the system, and assuming $\tau_s \omega_{\text{beat}} \ll 1$, gives the total rate of heat flow between tubes as

$$\dot{Q} = -\sum_i \tau_{s,i} \omega_{\text{beat},i}^2 \Delta q_i. \tag{3}$$

The sum is performed over all resonant pairs of modes between tubes and Δq_i is the difference in the energy between the pair, which for small thermal gradients may be approximated by the Bose distribution. If τ_s is assumed constant then the rate of exchange of heat depends on the square of the beat frequency of the coupled resonant pair, which in turn is dependent on the geometry of the coupling. A first order estimate for the beat frequency for the tubes considered in this work is obtained by assuming that $\kappa_{c,i} = \kappa_{\text{br}} \gamma \beta_i^2$, where β_i is the proportion of the motion of the ith mode that is in a radial direction and κ_{br} is the stiffness of the breathing mode. The largest contribution to energy transfer is made by the lowest frequency tube flattening mode, and we can define the "transmittance," $r_i = (\omega_{\text{beat},i}/\omega_{\text{beat,max}})^2$, relative to that for the flattening mode. Plotting r_i on a log-log scale (Fig. 4) reveals an inverse squared dependence on frequency. Furthermore, the total transmittance of all the modes combined is only $\sim$7.5 times that of the most efficiently transmitting mode, indicating that the bulk of the energy is transferred through a handful of key modes.

The energy transfer mechanisms described in this Letter, when considered together, give a picture of diffusionlike energy dissipation in composite nanomechanical systems. The findings from MD simulations are used to formulate a theoretical framework for describing nanoscale thermal transport. Rather than considering scattering of phonon wave packets (as with Boltzmann transport theory) the dissipation of an athermally populated phonon distribution and the transport of heat proceeds by exchange of energy between localized vibrational modes. As the options for energy transfer with other modes are limited at the nanoscale, the evolution of energy distribution (in both frequency and space) is similar to diffusion on a lattice. This model of nanoscale heat flow can be used to guide the engineering of new materials with novel thermal properties, for example, in understanding the thermal conduction percolation transition in nanotube composites and heat flow in nanoscale powders and fluid suspensions.

This work was performed under the auspices of the National Science Foundation by University of California Berkeley under Grant No. 0425914.

*Corresponding author.
Email address: jgrossman@berkeley.edu

[1] M. S. Dresselhaus and P. C. Eklund, Adv. Phys. **49**, 705 (2000).
[2] D. Li and A. Majumdar, *Annual Review of Heat Transfer* (Begell House, Redding, CT, 2005).
[3] S. Berber, Y.-K. Kwon, and D. Tománek, Phys. Rev. Lett. **84**, 4613 (2000).
[4] N. Mingo and D. A. Broido, Phys. Rev. Lett. **95**, 096105 (2005).
[5] L. G. C. Rego and G. Kirczenow, Phys. Rev. Lett. **81**, 232 (1998).
[6] J. Hone, M. Whitney, C. Piskoti, and A. Zettl, Phys. Rev. B **59**, R2514 (1999).
[7] C. Yu, L. Shi, Z. Yao, D. Li, and A. Majumdar, Nano Lett. **5**, 1842 (2005).
[8] D. W. Brenner, O. A. Shenderova, J. A. Harrison, S. J. Stuart, B. Ni, and S. B. Sinnott, J. Phys. Condens. Matter **14**, 783 (2002).
[9] B. Becker, P. K. Schelling, and S. R. Phillpot, Phys. Status Solidi C **1**, 2955 (2004).
[10] D. G. Cahill, W. K. Ford, K. E. Goodson, G. D. Mahan, A. Majumdar, H. J. Maris, R. Merlin, and S. R. Phillpot, Appl. Phys. Rev. **92**, 793 (2003).
[11] Measurements of CNT-polymer composites [12,13] have shown these networks to undergo a percolation transition in their electrical conductance, unaccompanied by a similar change in thermal conductance, indicating that electron transport contributes little to thermal transport.
[12] M. J. Biercuk, M. C. Llanguno, M. Radosavljevic, J. K. Hyun, A. T. Johnson, and J. E. Fischer, Appl. Phys. Lett. **80**, 2767 (2002).
[13] J.-M. Benoit, B. Corraze, S. Lefrant, P. Bernier, and O. Chauvet, Materials Research Society Symposium Proceedings **706**, Z3.28 (2002).
[14] This system was sufficient to reproduce the full phonon spectrum of the nanotubes.
[15] J. Kürti, V. Zólyomi, M. Kertesz, and G. Sun, New J. Phys. **5**, 125 (2003).
[16] G. Gao, T. Çagin, and W. A. G. III, Nanotechnology **9**, 184 (1998).
[17] D. A. Young and H. J. Maris, Phys. Rev. B **40**, 3685 (1989).
[18] E. T. Swartz and R. O. Pohl, Rev. Mod. Phys. **61**, 605 (1989).